NUCLEAR SCIENCE AND TECHNIQUES **25**, 020502 (2014)

Ordered water monolayer on ionic model substrates studied by molecular dynamics simulations*

SHAO Shi-Jing (邵士靖),[1,2] GUO Pan (郭盼),[1,2] ZHAO Liang (赵亮),[1,2] and WANG Chun-Lei (王春雷)[1,†]

[1] *Shanghai Institute of Applied Physics, Chinese Academy of Sciences, Shanghai 201800, China*
[2] *University of Chinese Academy of Sciences, Beijing 100049, China*

(Received January 8, 2014; accepted in revised form February 24, 2014; published online March 20, 2014)

The molecular behaviors of interfacial water molecules at the solid/liquid interface are of a fundamental significance in a diverse set of technical and scientific contexts, thus have drawn extensive attentions. On certain surfaces, the water monolayer may exhibit an ordered feature, which may result in the novel wetting phenomenon. In this article, based on the molecular dynamics simulations, we make a detailed structure analysis of the ordered water monolayer on ionic model surface with graphene-like hexagonal lattices under various charges and unit cell sizes. We carefully analyze the water density profiles and potential of mean force, which are the origin of the special hexagonal ordered water structures near the solid surface. The number of hydrogen bonds of the ordered water monolayer near the solid surface is carefully investigated.

Keywords: Ordered water monolayer, Hydrogen bond, Molecular dynamics simulations

DOI: 10.13538/j.1001-8042/nst.25.020502

I. INTRODUCTION

The complex behaviors of interfacial water [1–9], which are of great importance in research fields of protein stability and folding [10], molecular self-assembly [11], manipulating biomolecules [12], rearrangement of immunodeficiency virus [13] etc., have drawn extensive attentions [5–7, 14], since the molecular structure and dynamics of the interfacial water molecules are usually different from the bulk properties [15]. Interfacial water molecules play an important role in biophysical process. For example, water effectively catalyzes chiral interconversion of thalidomide [16], and dewetting transition promotes the amyloid fibrils formation [17]. Owing to the interaction between the interfacial water and the hydrophilic solid substrate, the diffusion of interfacial water [18] is slower, and the lifetime of hydrogen bonds [19] is longer, than that of the bulk water, as having been confirmed by experiments [20–22]. Recently, ordered structure of the interfacial water confined [23] at one or two dimensions has been studied extensively by both experimental and theoretical methods. In 2009, we reported a liquid water droplet on a water monolayer, termed as "ordered water monolayer does not completely wet water" on a model surface at room temperature [24]. Later, similar phenomena were observed by several experiments on sapphire c-plane electrolyte surface [25] and on self-assemble monolayer (SAM) surfaces with the $-$COOH terminal [26, 27]. In addition, theoretical simulations found similar phenomenon on hydroxylated metal oxide surfaces of Al_2O_3 and SiO_2 [4], Talc [28] and Pt(100) metal surfaces [29]. We also explored the effect of morphology [30] and the critical length of the charge dipoles of the solid surface [31] on the structures of interfacial water and the surface wetting behaviors.

In this article, based on molecular dynamics simulations, we investigate the structure and hydrogen bonds to show detail information of the ordered water monolayer on ionic model surface having graphene-like hexagonal lattices with various charges and unit cell sizes. The article is organized as follows. The ordered structure of water monolayer near the surface is described in Sec. III. A. In Sec. III. B, the water density and the potential of mean force (PMF) [28] are studied. In Sec. III. C, the number of hydrogen bonds is calculated to show the stable formation of hydrogen bonds network in the ordered water monolayer. Finally, a short conclusion is presented in the last section.

II. SIMULATION DETAILS

We configured a hexagonal solid lattice with 1664 solid atoms and the neighbor bond length l was described in Fig. 1, the same as our previous studies [24, 32]. The initial systems for the molecular dynamics simulations contained a water layer of about 4.0 nm thick on the ionic model surface, where positive and negative charges were located diagonally in neighboring hexagon, and it was found that the charge had great influence on the flux of water molecules in nanotube [12, 32]. All the simulations were performed at $T = 300$ K (NVT ensemble), with Gromacs 4.5.4 [34] by using a time step of 1.0 fs. The Lennard-Jones parameters of the solid atoms were $\varepsilon_{ss} = 0.105$ kcal/mol and $\sigma_{ss} = 33.343$ Å, and SPC/E water model [35] was used. The particle-mesh Ewald method [13] with a real space cutoff of 1 nm was adopted for the long-range electrostatic interactions and a 10 Å cutoff was used for the van der Waals interactions. The periodic boundary conditions were applied in three directions. The simulation time for every system was 4 ns and the last 2 ns data was collected for analysis.

Two series of simulations were performed to investigate the ordered water monolayer formation on a hexagonal

* Supported by the National Science Foundation of China (Nos. 11290164 and 11204341), the Knowledge Innovation Program of SINAP, the Knowledge Innovation Program of the Chinese Academy of Sciences, Shanghai Supercomputer Center of China and Supercomputing Center of Chinese Academy of Science

† Corresponding author, wangchunlei@sinap.ac.cn

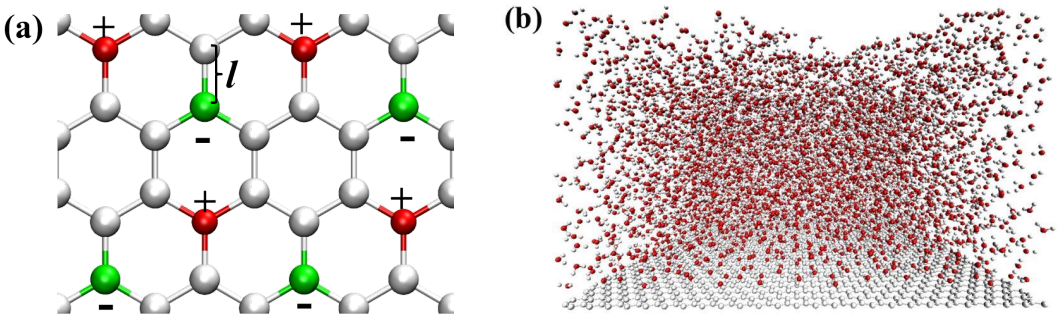

Fig. 1. (Color online) Hexagonal solid surface with charged pairs (a) and snapshot of the 4.0 nm thick water layer on the surface (b). The red and green spheres represent atoms with positive and negative charges, respectively, while neutral solid atoms are shown in white.

polarity solid surface. In the first series of simulations, the charge q of the solid atoms increased from 0.6 e to 1.0 e with 0.1 e interval and there were 5252 water molecules in the simulation boxes with the volume of 6.395 nm × 6.816 nm × 20.110 nm. The value of the neighboring bond length of solid atoms was kept as the constant of $l = 0.142$ nm. In the second series of simulations, the bond length l was set at 0.120 nm, 0.130 nm, 0.142 nm, 0.150 nm and 0.160 nm, with $q = 0.8$ e, and the water layer thickness was kept at about 4.0 nm, with the water molecules of 3525, 4314, 5252, 5721 and 6564, in the simulation boxes of 5.404 nm × 5.760 nm × 20.110 nm, 5.854 nm × 6.240 nm × 20.110 nm, 6.395 nm × 6.816 nm × 20.110 nm, 6.755 nm × 7.20 nm × 20.110 nm and 7.205 nm × 7.680 nm × 20.110 nm, respectively.

III. RESULTS AND DISCUSSIONS

A. Structure analysis of the water monolayer

To study the structure of water molecules in the water monolayer on the solid surface, two angle parameters θ and φ are introduced as illustrated in Fig. 2(c) and 2(d), where θ is defined as the angle between a water molecule dipole and z axis, and φ is the angle formed between the projection onto x-y plane of a water dipole and a crystallographic direction [30]. Here, the definition of the water monolayer is the water molecules in the first layer next to the solid surface with an average thickness of 0.4 nm, the same as our previous work [24], which is also consistent with the existence of an experimentally observable monolayer [36]. The second layer is defined as the water molecules with an average thickness of 0.4 nm above the water monolayer.

As shown in Fig. 2(e), two peaks of angle θ confirm the two states, namely, state 1 and state 2 as depicted in Figs. 2(a) and 2(b). The left peaks at $\theta \approx 60^\circ$ represent state 1 with oxygen atoms attracted by the positive charged atoms, while the right peaks at $\theta \approx 120^\circ$ represent state 2 with −OH bonds pointing towards the negative charged atoms. Fig. 2(f) is the normalized probability distributions of angle φ with three peaks at $\varphi \approx 0^\circ$, 120° and 240°, which demonstrate that the water molecules in the monolayer can form a 2D hexagonal configuration (Fig. 2(d)), the same as our previous work [24]. As q increases from 0.6 e to 1.0 e, all the peaks in Figs. 2(e) and 2(f) become higher and the water molecules in the monolayer become ordered due to the larger binding of the surface charged atoms. However, the peaks are quite different as the bond length l increases. At $l = 0.142$ nm and $q = 0.8$ e, the peaks are the highest (Figs. 2(g) and 2(h)), hence the most ordered water molecules in the water monolayer. As the l departs from 0.142 nm, the ordered hexagonal water monolayer gradually disappears. These results show that the ordered water structure greatly depends on the surface charge and suitable cell size.

B. Water density distribution profiles and PMF curves

Figures. 3(a) and 3(b) show the water density as a function of z at different q and l. The reference $z = 0$ corresponds to the solid surface. Two peaks can be seen for all curves locating at $z = 0.3$ nm and 0.6 nm. Due to the strong binding of charges on the surface, we can observe a quite high density peak near the solid surface forming the monolayer. The density increases with the charge, reaching the largest at $q = 0.9$ e and 1.0 e. With increasing cell size, the density increases first until $l = 0.142$ nm, where it begins to decrease, indicating the formation and break-down of the ordered structure, respectively.

The density relates to potential of mean force (PMF), F (z), by the expression [28],

$$F(z) = -k_B T \ln(\rho(z)/\rho_w), \quad (1)$$

where, k_B is the Boltzmann constant and $\rho_w = 33\,\mathrm{nm}^{-3}$ is the number density of bulk water. $F(z)$ is the potential of

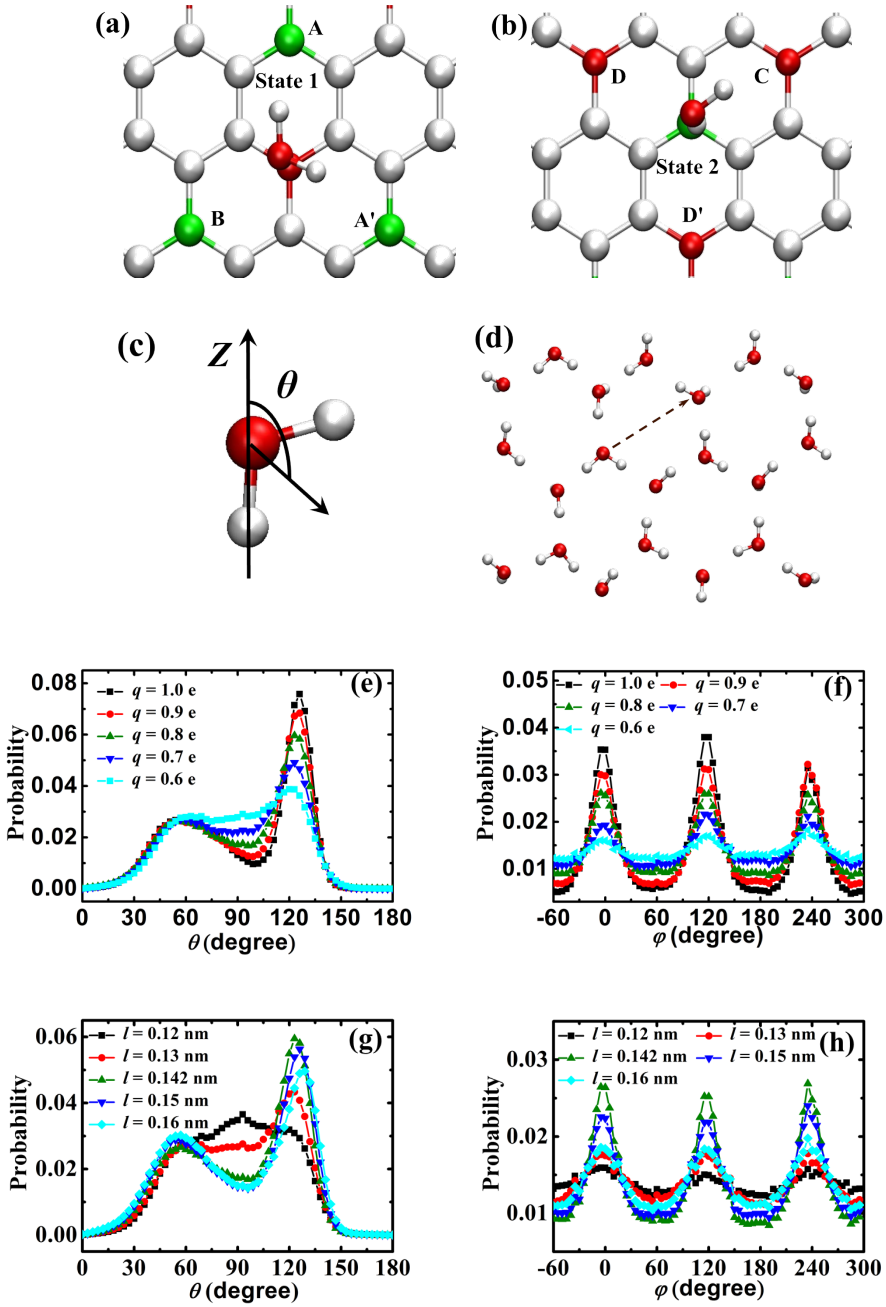

Fig. 2. (Color online) (a) State 1 with water molecule adsorbed by positive binding charge and three negative neighbor charges marked with A, A', B. (b) State 2 with water molecule adsorbed by negative binding charge and three positive neighbor charges marked with C, D, D'. (c) Schematic of angle θ defined as the angle between a water molecule dipole and z axis. (d) Schematic of angle φ defined as the angle formed between the projection onto x-y plane of a water dipole and a crystallographic. (e) Probability distribution of θ in the monolayer *vs.* q. (f) Probability profile for angle φ in the monolayer *vs.* q. (g) Probability profiles of θ in the monolayer *vs.* l. (h) Probability distribution of φ in the monolayer *vs.* l.

mean force for bringing a water molecule from the bulk to a distance z from the solid surface. Figs. 3(c) and 3(d) show the PMF curves and for every curve there are two valleys at $z = 0.3$ nm and 0.6 nm. The two valleys account for the adsorption of the solid surface. The minimum PMF at $z = 0.3$ nm is about -0.9 kcal/mol at $q \geq 0.8$ e and $l = 0.142$ nm. The PMF reveals the adsorption interaction of the solid surfaces at the valleys. The adsorption increases with the charge, displaying a wide range of binding strength to attract the water molecules and form the ordered monolayer. This is different from the bulk water. Suitable cell size is quite important for adsorption interaction of the solid surface and formation of

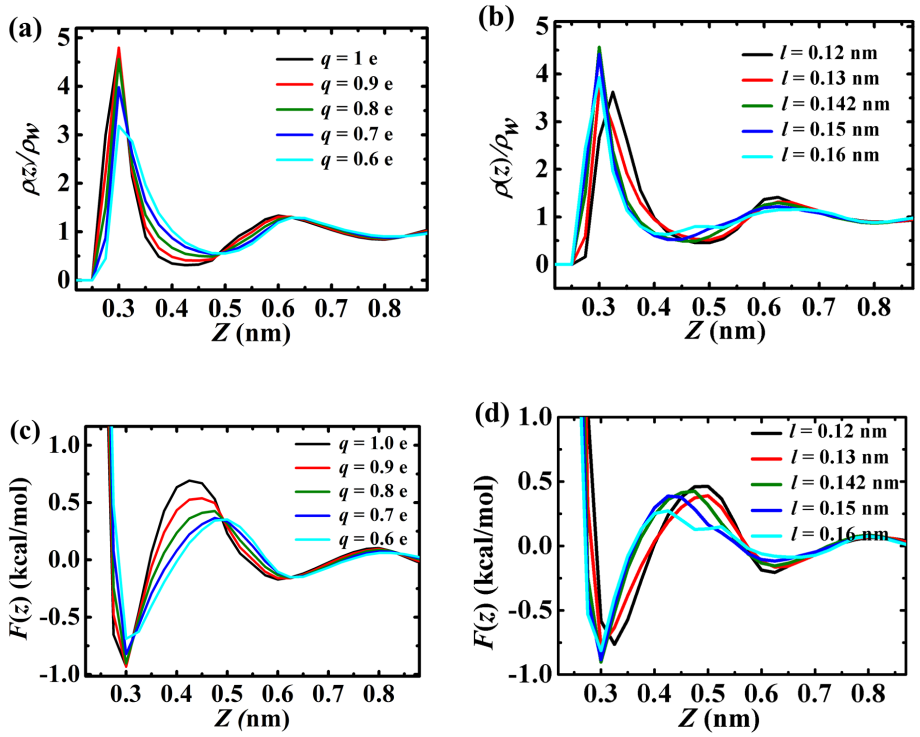

Fig. 3. (Color online) (a) Density profile of water molecules away from the surface *vs.* q, divided by the number density of bulk water, $\rho_w = 33\,\mathrm{nm}^{-3}$. (b) The density profile *vs.* l, ρ_z/ρ_w. (c) Potential of mean force F (z) *vs.* q. (d) $F(z)$ *vs.* l.

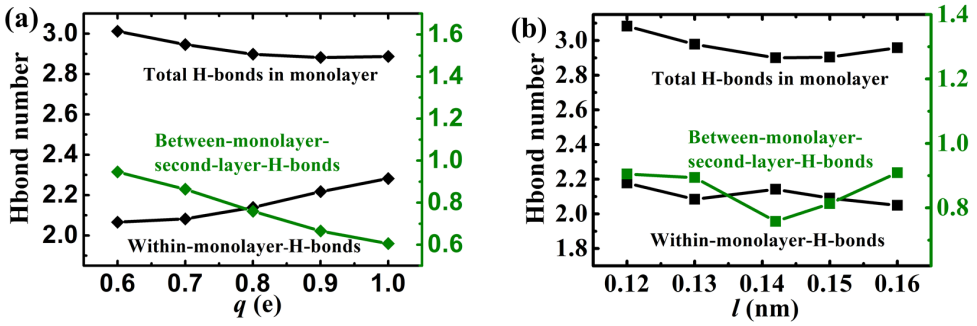

Fig. 4. (Color online) Average number of hydrogen bonds of a water molecule to other water molecules in the same layer (♦), to water molecules in the second layer (●), and their sum (■) as function of q (a) and l (b).

the monolayer. The PMF results indicate that the distribution of water molecules and formation of the ordered water monolayer are affected by the charge and cell size.

C. Hydrogen bonds in the water monolayer

The ordered water monolayer affects the formation of hydrogen bonds of the water molecules in the interface. We calculated the average hydrogen bonds of a water molecule to its neighboring water molecules in the same monolayer ("in the monolayer" H bonds), and to water molecules in the second layer ("to the second layer" H bonds), as shown in Fig. 4. The criteria characterizing existence of hydrogen bond between two water molecules is the geometric definition that their O−O distance is less than 3.5 Å and simultaneously the angle H−O · · · O is less than 30° [37].

In Fig. 4(a), the number of hydrogen bonds within the monolayer increases and the number of the hydrogen bonds between the monolayer and the second layer decreases as the increase of charge. Their sum remains at $\sim$ 2.9 when $q \geq 0.8\,\mathrm{e}$, which approaches 3, the maximum number of hydrogen bonds that any water molecule can form in the monolayer [24]. The interaction energy between the monolayer and the charged surface is stronger when the charge increases as we calculate in Sec.III(B). The water molecules bound in

the monolayer make it easy to form hydrogen bond with the water molecule in the same layer. There is competition for formation of hydrogen bonds between the "in the monolayer" H bonds and "to the second layer" H bonds. The increase of former leads to the decrease of latter for weaker interaction between the water molecules in the monolayer and water molecules in the second layer. In Fig. 4(b), when $l = 0.142\,\text{nm}$ and $q = 0.8\,\text{e}$, the average number of hydrogen bonds among the water molecules in the monolayer is larger than the others, and the number of hydrogen bonds between the monolayer and the second layer is the smallest. The total number of hydrogen bonds per water molecule in the monolayer is also about 3. Thus, the large charge and the suitable unit cell size ($l = 0.142\,\text{nm}$) make the water molecules in the monolayer prefer to form hydrogen bonds within the water monolayer, rather than form hydrogen bonds between the monolayer and water molecules in the second layer. Clearly, the unit cell size is also the key to the formation of hydrogen bonds of the water molecules near the solid surface.

IV. CONCLUSION

In summary, we study the structure, properties of free energy and hydrogen bonds of ordered water monolayer on ionic model surface with graphene-like hexagonal lattices with different charges and unit cell sizes by molecular dynamics simulations. The results indicate that both the charge and unit cell size have a great effect on the water molecular behaviors in the monolayer, such as water molecular configurations and the hydrogen bond network. The charged surface displaying strong adhesive interaction is described by the water density profiles and potential of mean force. We have also carefully investigated the number of hydrogen bonds of the ordered water monolayer near the solid surface. It is expected that the finding in this paper may help to deeply understand the ordered water monolayer on the surface.

ACKNOWLEDGEMENTS

We thank Prof. FANG Hai-Ping and Dr. XIU Peng for the helpful discussions and suggestions.

[1] Stirnemann G, Rossky P J, Hynes J T, *et al*. Faraday Discuss, 2010, **146**: 263–281.
[2] Stirnemann G, Castrillón S R V, Hynes J T, *et al*. Phys Chem Chem Phys, 2011,**13**: 19911–19917.
[3] Malani A and Ayappa K G. J Chem Phys, 2012, **136**: 194701.
[4] Phan A, Ho T A, Cole D R, *et al*. J Phys Chem C, 2012, **116**: 15962–15973.
[5] Ostroverkhov V, Waychunas G A, Shen Y R. Phys Rev Lett, 2005, **94**: 46102.
[6] Zheng J M, Chin W C, Khijniak E, *et al*. Adv Colloid Interfac, 2006, **127**: 19–27.
[7] Sovago M, Campen R K, Wurpel G W H, *et al*. Phys Rev Lett, 2008, **100**: 173901.
[8] Zanotti J M, Bellissent-Funel M C, Chen S H. Europhys Lett, 2005, **71**: 91–97.
[9] Goertz M P, Houston J, Zhu X Y. Langmuir, 2007, **23**: 5491–5497.
[10] Hummer G, Garde S, Garcıa A E, *et al*. Chem Phys, 2000, **258**: 349–370.
[11] Vauthey S, Santoso S, Gong H, *et al*. P Natl Acad Sci USA, 2002, **99**: 5355–5360.
[12] Xiu P, Zhou B, Qi W P, *et al*. J Am Chem Soc, 2009, **131**: 2840–2845.
[13] York D M, Darden T A, Pedersen L G, *et al*. Biochemistry-US, 1993, **32**: 1443–1453.
[14] Gragson D E, McCarty B M, Richmond G L. J Am Chem Soc, 1997, **119**: 6144–6152.
[15] Bandyopadhyay S, Tarek M, Klein M L. Curr Opin Colloid Int, 1998, **3**: 242–246.
[16] Tian C, Xiu P, Meng Y, *et al*. Chem-Eur J, 2012, **18**: 14305–14313.
[17] Yang Z, Shi B, Lu H, *et al*. J Phys Chem B, 2011, **115**: 11137–11144.
[18] Chen S H, Gallo P, Bellissent-Funel M C. Can J Phys, 1995, **73**: 703–709.
[19] Li J, Liu T, Li X, *et al*. J Phys Chem B, 2005, **109**: 13639–13648.
[20] Riter R E, Willard D M, Levinger N E. J Phys Chem B, 1998, **102**: 2705–2714.
[21] Pal S K, Peon J, Bagchi B, *et al*. J Phys Chem B, 2002, **106**: 12376–12395.
[22] Pal S K, Peon J, Zewail A H. P Natl Acad Sci USA, 2002, **99**: 1763–1768.
[23] Pal S, Balasubramanian S, Bagchi B. J Phys Chem B, 2003, **107**: 5194–5202.
[24] Wang C, Lu H, Wang Z, *et al*. Phys Rev Lett, 2009, **103**: 137801.
[25] Lützenkirchen J, Zimmermann R, Preočanin T, *et al*. Adv Colloid Interfac, 2010, **157**: 61–74.
[26] James M, Darwish T A, Ciampi S, *et al*. Soft Matter, 2011, **7**: 5309–5318.
[27] James M, Ciampi S, Darwish T A, *et al*. Langmuir, 2011, **27**: 10753–10762.
[28] Rotenberg B, Patel A J, Chandler D. J Am Chem Soc, 2011, **133**: 20521–20527.
[29] Limmer D T, Willard A P, Madden P, *et al*. P Natl Acad Sci USA, 2013, **110**: 4200–4205.
[30] Wang C, Zhou B, Xiu P, *et al*. J Phys Chem C, 2011, **115**: 3018–3024.
[31] Wang C, Zhou B, Tu Y, *et al*. Sci Rep, 2012, **2**:358.
[32] Ren X P, Zhou B, Li L T, *et al*. Chin Phys B, 2013, **22**: 016801.
[33] Xu W, Tu Y, Wang C, *et al*. Nucl Sci Tech, 2011, **22**: 307–310.
[34] Hess B, Kutzner C, van der Spoel D, *et al*. J Chem Theory Comput, 2008, **4**: 435–447.
[35] Berendsen H J C, Grigera J R, Straatsma T P. J Phys Chem, 1987, **91**: 6269–6271.
[36] Miranda P B, Xu L, Shen Y R, *et al*. Phys Rev Lett, 1998, **81**: 5876–5879.
[37] Luzar A and Chandler D. J Chem Phys, 1993, **98**: 8160–8173.